THIRD EUROPEAN ROTORCRAFT AND POWERED LIFT AIRCRAFT FORUM

Paper No. 6

DEVELOPMENT OF LINEAR AND NONLINEAR HUB SPRINGS FOR TWO-BLADED ROTORS

J. DREES, L. DOOLEY, B. BLANKENSHIP

BELL HELICOPTER TEXTRON

FORT WORTH, TEXAS, USA

September 7-9, 1977

AIX-EN-PROVENCE, FRANCE

ASSOCIATION AERONAUTIQUE ET ASTRONAUTIQUE DE FRANCE

DEVELOPMENT OF LINEAR AND NONLINEAR HUB SPRINGS FOR TWO-BLADED ROTORS

J. M. Drees
Director of Technology

L. W. Dooley
Senior Stability and Control Engineer

B. L. Blankenship
Technology Staff Engineer

Bell Helicopter Textron
Fort Worth, Texas

Abstract

Advanced two-bladed rotor systems may have hub springs for improved control and stability. The paper will discuss the results of early tests with locked-out flapping hinge (very stiff hub spring), followed by the introduction of metal torsion hub springs, culminating in recent flight tests with linear and nonlinear elastomeric hub springs, as applied to the Bell Models 222 and 214ST. The elastomeric hub springs have demonstrated enhanced handling qualities and reduced pilot workload, improved low-g capability, and increased center of gravity range with little degradation in fuselage vibration or rotor component life. The paper concludes with speculations concerning the feasibility of the most simple of all rotor systems: the bearingless two-bladed rotor.

Notation

a = lift curve slope

a_1 = longitudinal component of flapping

c = rotor blade chord

C_P = pylon damping constant

C_B = flap damping constant

g = gravitational constant

h = height of hub above helicopter cg

I_B = rotor flapping inertia

I_P = pylon inertia about base (rotor mass included)

$I_{B/P}$ = inertia ratio: I_B/I_P

I_{FUS} = helicopter pitch inertia

K_B = hub spring constant

K_P = pylon spring constant

q = helicopter pitch rate

Q_x = external moment in the θ_x direction

Q_y = external moment in the θ_y direction

Q_β = external moment in the β direction

R = rotor radius

T = rotor thrust

V = helicopter airspeed

β = rotor flapping relative to mast

γ = Lock Number: $\frac{\rho a c R^4}{I_B}$

$\delta_{F/A}$ = pilot longitudinal control deflection

ξ_B = flap damping ratio: $C_B/(2\omega_B I_B)$

ξ_P = pylon damping ratio: $C_P/(2\omega_P I_P)$

ρ = air density

σ = system damping for mode with natural frequency ω

θ_x = angular deflection of the pylon in a direction parallel to B

θ_y = angular deflection of the pylon in a direction perpendicular to B

Ω = rotational frequency

ω = system natural frequency

ω_B = flapping frequency: $\sqrt{(K_B/I_B)}$

ω_P = pylon frequency: $\sqrt{(K_P/I_P)}$

$\omega_{B/P}$ = frequency ratio: ω_B/ω_P

Introduction

For light and medium helicopters, the Bell two-bladed rotor has proved to be a successful concept. Its strong points as listed by Kelley in Reference 1 are simplicity, ruggedness, absence of ground resonance, low vibration at low speeds and in flares, easy parking, and low cost. In the past its list of weaknesses included noise, vibrations at high speed, and reduced control power in high speed push-overs.

Recent developments have resulted in improvements aimed at mitigating or eliminating the weak points without adversely affecting the advantages of the two-bladed rotor. For instance, low tip speeds used in the JetRanger, LongRanger, and Model 222 helicopters reduced the rotor noise. The introduction of a nodalized-focal pylon suspension system has resulted in low and comfortable cabin vibration levels in the .05 to .10g two-per-rev levels for the Bell Helicopter Models 214, 206L and 222 throughout the speed range and in maneuvers.

Elimination of the third weakness, reduced control power in high speed push-overs, requires some kind of hub restraint to provide a hub moment as a function of rotor flapping. The reason for this is that the lateral control moment of a teetering rotor about the center of gravity of the aircraft becomes small at low values of rotor thrust. Exploration of the feasibility of hub restraint for a two-bladed rotor was initiated shortly after Bell conducted the first successful rigid three-bladed rotor experiments in 1959, and the subject has been under study ever since. The newest Bell products with two-bladed rotors (222, 214ST) have hub springs as standard equipment.

In this paper, results of tests and analyses and considerations that led to the development of hub springs are discussed. The paper will conclude with speculations concerning the feasibility of a rigid-type two-bladed rotor in which flapping hinges and hub springs are eliminated altogether.

I. Test with Flapping Hinge Locked Out

Shortly after successfully demonstrating the feasibility of three-bladed experimental rigid rotors in 1959 on a Model 47 helicopter (Reference 2), the idea of trying a rigid two-bladed rotor was advanced. This was simply done by locking out the gimbal, and in 1961 a tie-down test run was made. The following excerpt is taken from the pilot's report of this test:

> During this ground run, as rotor rpm was being increased to engage the clutch, the pylon rotor system entered an unstable whirling frequency. This occurred while oscillograph records were being taken. It was determined from these records that the frequency was 1/rev with the rotor at 164 rpm. Although the vibration resulting from the instability was quite violent, no damage to the helicopter was detected. The configuration was a two-bladed rigid to the mast rotor, and standard pylon suspension for a 47G.

As indicated in the report, limited instrumentation on board the helicopter showed that the pylon was excited at one per rev near the pylon natural frequency. The pylon showed little one per rev during the run-up, but after the one per rev developed, it remained for quite some time while rpm was reduced as rapidly as possible. No pictures of the installation were taken, because the lock-out device was removed after this experiment. A simple test the next day with a T bar in a drill motor (see Figure 1) convinced us that we had run into a hereto unexperienced whirl instability associated with a very rigid two-bladed rotor.

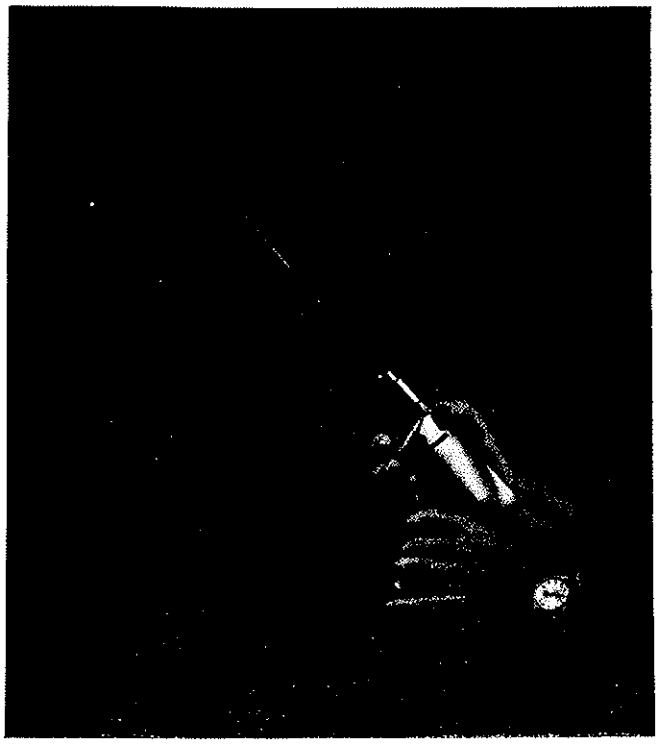

Figure 1. Simple Pylon Instability Model

Subsequent model tests with rotor blades installed and a hub in which flapping spring could be varied in stiffness from 0 to ∞ provided more detailed information. With reduced flapping spring stiffness, the system became stable, although more responsive to out of track than the freely teetering rotor. This stands to reason since the hub spring will transmit a one per rev moment into the pylon.

In the next chapter a simple stability analysis is presented in which pylon and hub restraints as well as terms for both damping of the pylon and in the flapping axis are included.

II. Pylon Stability as a Function of Hub Spring Stiffness

A simple analytical model can be used to show that pylon stability is maintained for a two-bladed rotor with hub springs by a reasonable amount of pylon damping. The analytical representation consists of two rigid bars: P, for the pylon, and B, for the two-bladed rotor. The bars are connected by springs and dampers as shown in Figure 2. The rotation is about a fixed axis.

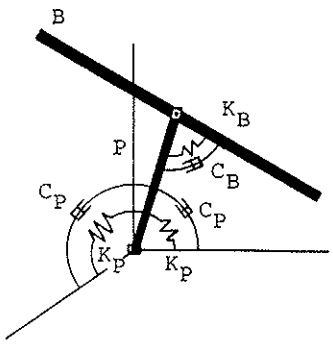

a. Model

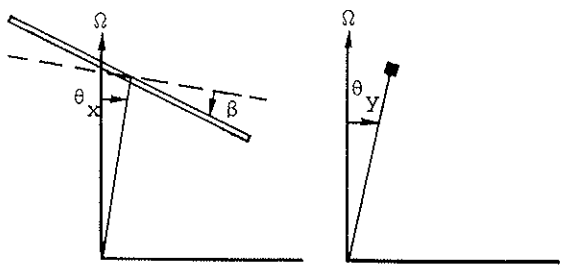

b. Coordinate Axes

Figure 2. Two-Bladed Rotor and Pylon Model

The equations of motion, in rotating coordinates, are:

$$I_P(\ddot{\theta}_x - \Omega^2\theta_x - 2\Omega\dot{\theta}_y) + K_P\theta_x + C_P(\dot{\theta}_x - \Omega\theta_y) - C_B\dot{\beta} - K_B\beta = Q_x \quad (1)$$

$$I_P(\ddot{\theta}_y - \Omega^2\theta_y + 2\Omega\dot{\theta}_x) + K_P\theta_y + C_P(\dot{\theta}_y + \Omega\theta_x) = Q_y \quad (2)$$

$$I_B[(\ddot{\beta}+\ddot{\theta}_x) + \Omega^2(\beta+\theta_x)] + C_B\dot{\beta} + K_B\beta = Q_\beta \quad (3)$$

The stability determinant can be derived by assuming solutions of the form $x = x_o e^{st}$:

$$\begin{vmatrix} s^2+2\xi_P\omega_P s + (\omega_P^2-\Omega^2) & -2\Omega s - 2\xi_P\omega_P\Omega & -2I_{B/P}\xi_B\omega_B s - I_{B/P}\omega_B^2 \\ 2\Omega s + 2\xi_P\omega_P\Omega & s^2+2\xi_P\omega_P s + (\omega_P^2-\Omega^2) & 0 \\ s^2+\Omega^2 & 0 & s^2+2\xi_B\omega_B s + (\omega_P^2+\Omega^2) \end{vmatrix} = 0 \quad (4)$$

The roots of the polynominal obtained from (4) are of the form

$$s = \sigma + i\omega$$

so that the coefficient of the imaginary component is the coupled natural frequency of a mode and the coefficient of the real component indicates damping in the mode. The condition for stability is $\sigma < 0$.

If the elements of the stability determinant are normalized on the pylon frequency, ω_P, the remaining parameters are

$I_{B/P}$, the inertia ratio

$\omega_{B/P} = \frac{\omega_B}{\omega_P}$, the rotor flapping frequency

ξ_P and ξ_B, the damping coefficients.

For zero hub spring, $\omega_{B/P} = 0$, and no damping, the frequency versus Ω plots in rotating coordinates are just straight lines (see dotted lines in Figure 3):

$$\frac{\omega}{\omega_P} = \frac{\Omega}{\omega_P} \qquad (5)$$

$$\frac{\omega}{\omega_P} = 1 + \frac{\Omega}{\omega_P} \qquad (6)$$

$$\frac{\omega}{\omega_P} = \left| 1 - \frac{\Omega}{\omega_P} \right| \qquad (7)$$

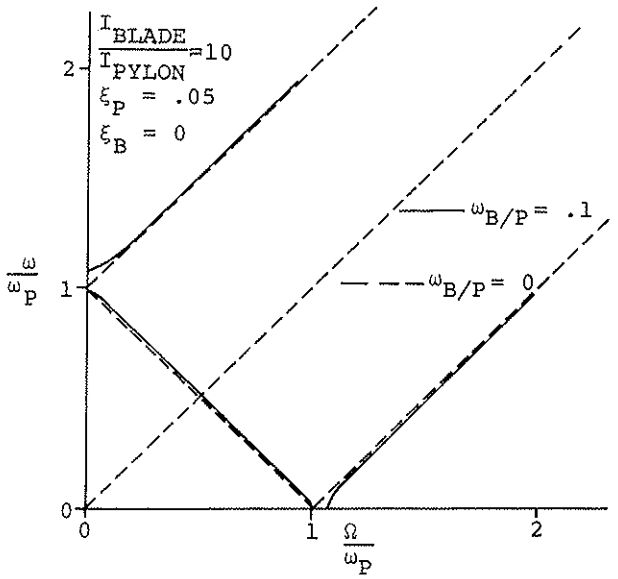

Figure 3. Coleman Diagram for Two-Bladed Rotor and Pylon Model

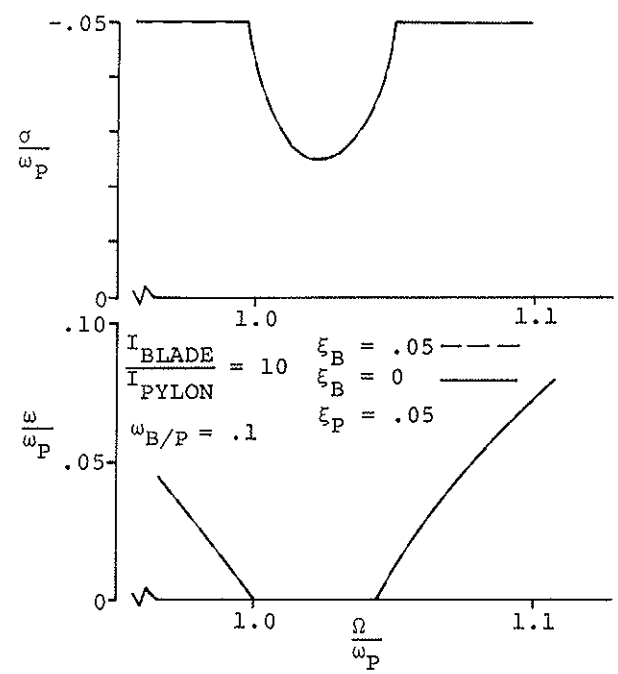

Figure 4. Mode Damping for Two-Bladed Rotor and Pylon Model

(5) is the expected one-per-rev flapping mode. (6) is the pylon advancing mode and (7) the pylon retreating mode. For this case there is no question of stability. However, as $\omega_{B/P}$ is increased, a gap appears to the right of $\frac{\Omega}{\omega_P} = 1$. This is the region of a possible whirl instability. The frequency, in rotating coordinates, is zero, and stability depends on the presence of pylon damping, the inertia ratio $I_{B/P}$, and the hub spring constant or, as it appears here, on $\omega_{B/P}$. Figure 3 (solid) lines) shows results from (4) for $\xi_P = .05$, $I_{B/P} = 10$, $\omega_{B/P} = .1$. In Figure 4 the gap region is blown up to show more precisely the zero-frequency interval, and the mode damping is plotted versus rotational speed. Variations of flap damping do not affect this mode.

A realistic range for the inertia ratio, based on BHT Models 209 and 206B is 6.0-8.0. To achieve desired increase in control power and hover stability, ξ_P should be as high as .05. Reasonable pylon damping that can be obtained from mechanical dampers ranges up to 10% of critical. Parameter sweeps showed that whirl mode damping decreases:

- with increasing hub spring constant
- with increasing inertia ratio
- with decreasing pylon damping constant.

Stability boundary points (i.e., $\sigma = 0$) occurred for the combinations:

$$\omega_{B/P} = .214,\ I_{B/P} = 10,\ \xi_P = .10$$

$$\omega_{B/P} = .2,\ I_{B/P} = 7,\ \xi_P = .05$$

$$\omega_{B/P} = .2,\ I_{B/P} = 10,\ \xi_P = .09$$

The strongest factor is flapping frequency. There is an indication that a rule for proper design may be derived in simple form, such as:

$$(\omega_{B/P})^3 \cdot \frac{I_{B/P}}{\xi_P} < 1 \qquad (8)$$

The case shown in Figure 4 has all three parameters on the destabilizing limits of ranges considered reasonable, but stability is retained. For this case, (8) is:

$$(.1)^3 \cdot \frac{10}{.05} = .2 < 1$$

The effect of flap damping ζ_B was also investigated. Within practical limits, the influence of ζ_B on whirl stability was found to be negligible. This is shown also in Figure 4.

III. Test Results with Metal Hub Springs

Flight Test

Figure 5 shows a torsional hub spring installed on a UH-1B helicopter. Two spring rates were tested, 1250 ft-lbs/degree/rotor and 2500 ft-lbs/degree/rotor.

At the time (1965) these tests were done, there was not yet customer interest in achieving low-g maneuver capability. The main objective was to explore pylon stability, possible increase in cg envelope, and, most of all, the effect of the hub spring on vibrations.

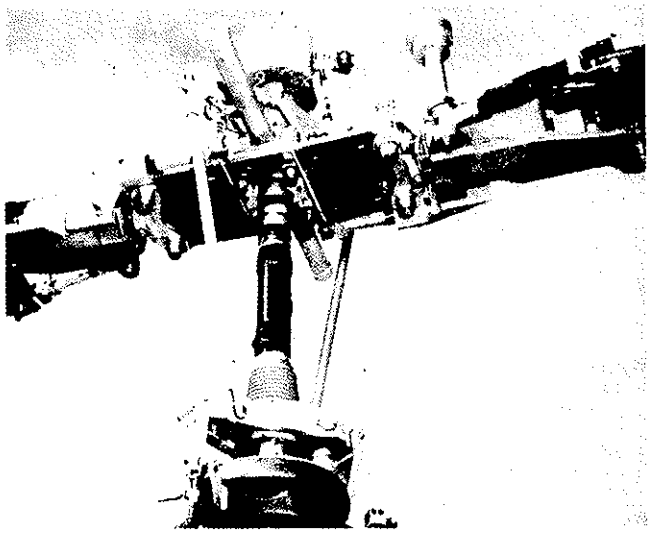

Figure 5. Metal Hub Spring Installed on Model UH-1B

The test results shown in Figure 6 demonstrated that a measurable increase in hover control power was achieved, indicated by the reduced stick travel with cg location. The pylon was stable for both springs, but the two-per-rev vibration levels were increased to unacceptable levels. An example of this increase is shown in Figure 7. An unacceptable increase in two per rev of about .2 g's at high speed was measured.

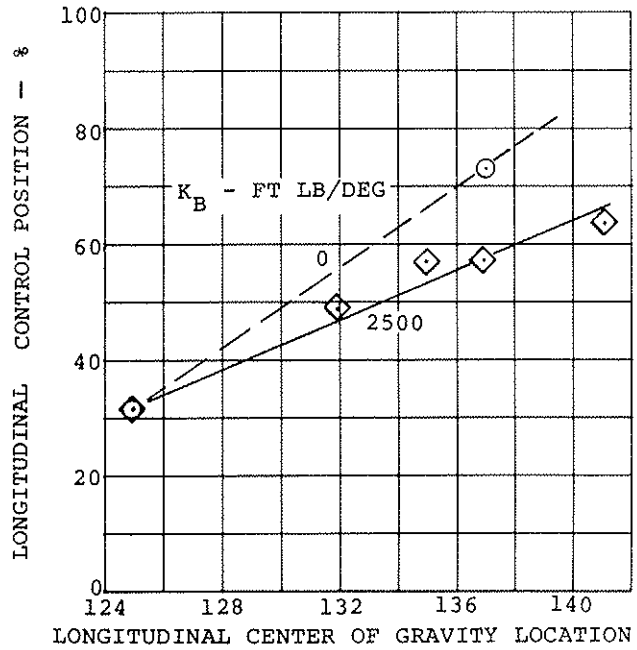

Figure 6. Effect of Hub Spring on Hovering Control Positions

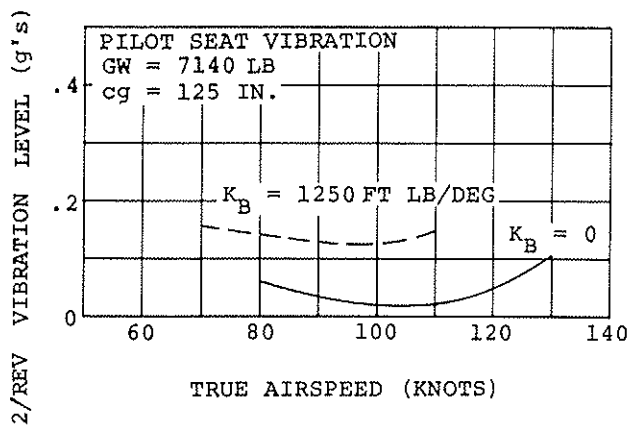

Figure 7. Effect of Hub Spring on Pilot Seat Vibration

It needs to be pointed out that the mast moment due to the flapping spring as seen by the rotor and the mast is two times the average hub moment on the non-rotating mast. This, of course, is due to the two-per-rev character of the moment generated by rotor flapping. The stiffer the spring, the higher the two-per-rev input. This two-per-rev input is the reason that the vibration levels went up in the first tests on the UH-1 helicopter and gave rise to a series of studies aimed at reducing vibration levels as discussed next.

Vibration Reduction

Essentially three ways were explored to reduce fuselage vibrations due to hub moments:

(a) Focused pylon. It was found (Reference 4) that there exists one unique focal point on the mast in which both hub inplane shear forces and hub moments are isolated. Figure 8 shows an example. It is seen that by focusing at point A, with the spring rate K_p, perfect isolation is achieved. Unfortunately, at this point the pylon is at two-per-rev resonance and A is the nodal point of the resonant mode. It is very unlikely that a resonant pylon even with enough damping can be used, although this has not been verified by testing.

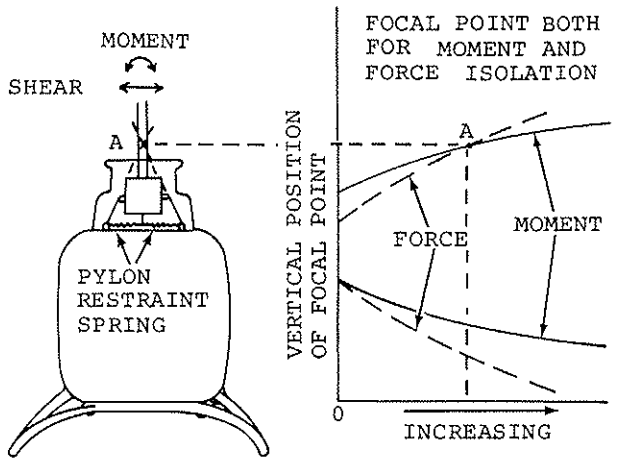

Figure 8. Focused Pylon Force and Moment Isolation

(b) Underslinging. By the choice of the proper underslinging, the magnitude of the oscillation moment about the pylon pivot point B of Figure 9 can be changed. It appears that, as shown by Sonneborn and Yen (Reference 5), that one can set $F \times (l+u) - M = 0$ and find the optimum underslinging for low vibration. This optimum underslinging is found to be slightly higher in the case of a hub spring than for the standard case without a hub spring. This was confirmed by model tests. Variations in underslinging were also tested full scale on the OH-58A rotor, but these tests did not reveal any difference in vibration level due to the amount of underslinging. This was only understood later when further calculations

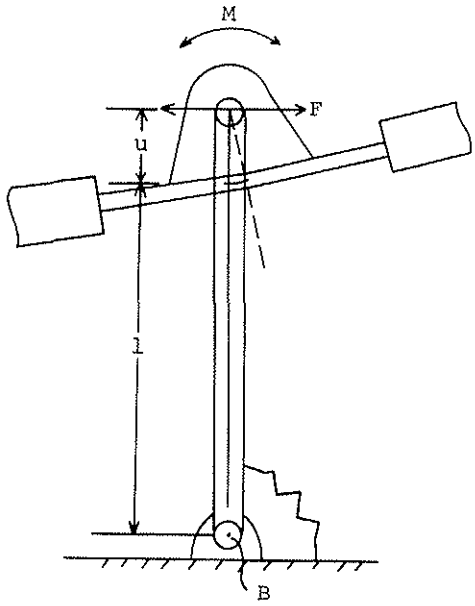

Figure 9. Focused Pylon with Underslung Rotor

were made which included the first inplane blade frequency as explained next under (c).

(c) Inplane cantilever blade frequency. In Reference 5 it is explained that when the analysis includes the first inplane blade mode, the underslinging has to be adjusted for the inplane blade motions in order to achieve minimum pylon response about the pivot point B of Figure 9. It was consequently discovered that if the inplane cantilever blade frequency (no hub mobility) is placed at exactly one per rev, then the underslinging for lowest vibration becomes independent of the hub spring stiffness. Figure 10 illustrates this. Figure 11 shows the test model used to investigate this effect experimentally. This is an important finding because it permits the use of much stiffer hub springs than originally thought possible.

The reason for this phenomenon is quite simple: the blade acts like a dynamic absorber to the mast. Any tendency for the mast to oscillate at two per rev (nonrotating) [= one per rev (rotating)] is stopped by the rotor acting as a Frahm damper. The fact that the inplane cantilever frequency is exactly at one per rev is no problem because the inplane blade frequency couples with the pylon to give a coupled frequency of greater than 1, say 1.3 per rev. In fact, this

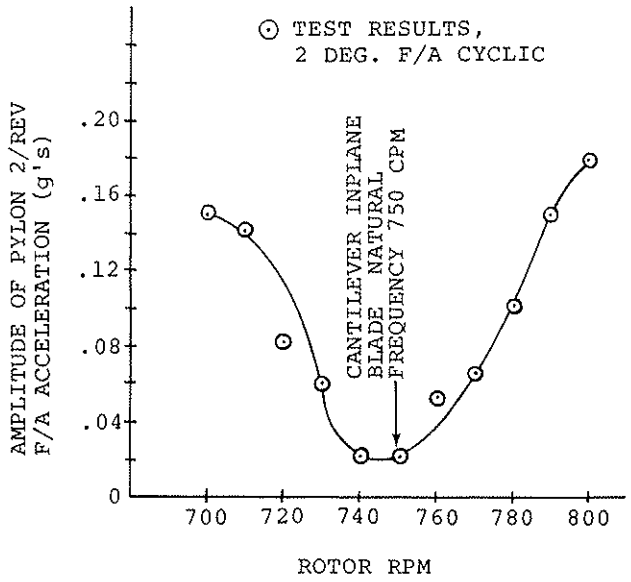

Figure 10. Pylon Vibration as a Function of Rotor RPM

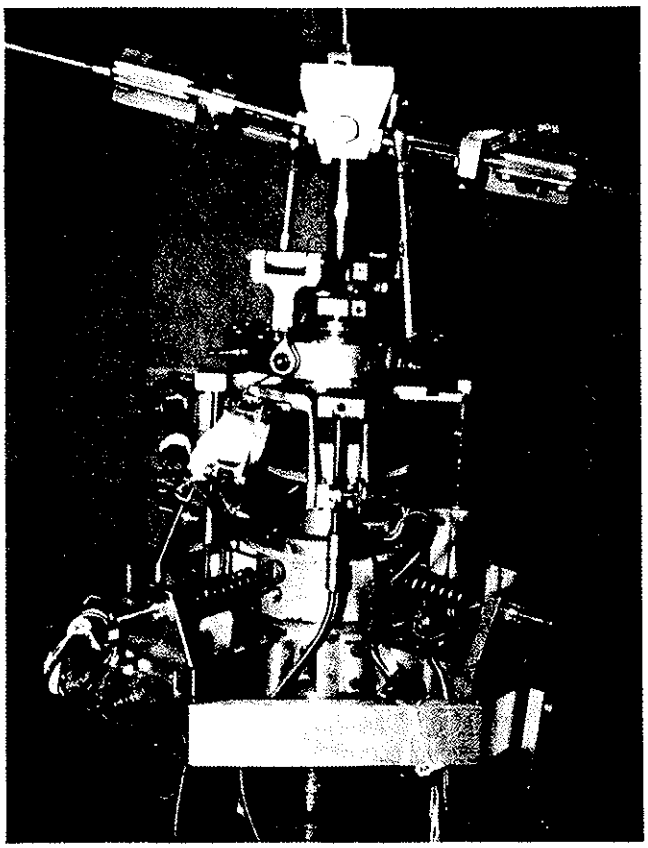

Figure 11. Rotor and Pylon Test Model

describes the frequency placement of the OH-58 and 206 helicopters and might explain why the test where the underslinging was changed did not result in a variation in vibration levels.

Tests With Improved Pylon Systems

About a decade ago, with the advent of new military requirements for more positive control power up to negative .5 g's, the interest in hub springs renewed. Meanwhile, improved vibration isolation systems had been developed, thus giving hope that hub springs could be installed without undue increase in vibrations. The same type of metal hub spring as shown in Figure 5 was tested on both the Model 206/OH-58 and on the KingCobra. Both helicopters have a focused pylon which gives very good isolation for inplane rotor forces. The KingCobra was additionally equipped with a nodal beam installation.

The results of these tests were very encouraging. Figure 12 shows the two-per-rev vibration level of the KingCobra pilot and gunner seats. As is shown, the vibration levels are with and without hub springs in the order of 0.05 g's and would meet the new Army requirements. Low-g flights were also executed. Control power under low-g conditions was clearly enhanced by the hub springs.

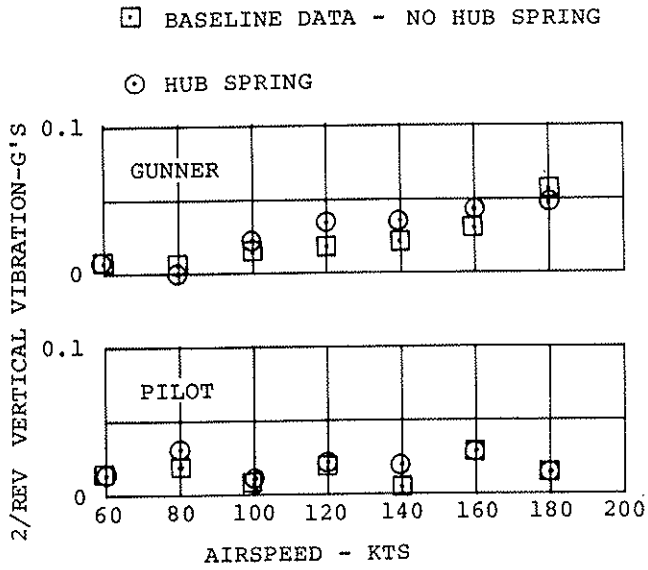

Figure 12. KingCobra Vibration Characteristics

The tests on the Model 206/OH-58 included evaluation of the effect of varying spring rates. At first, a low spring rate (10% increase in hovering control power) provided by an elastomeric flapping bearing was used in a low-g maneuverability test. Sustained zero-g levels were attained with this helicopter as shown in Figure 13 (from Reference 3). Later tests, using a torque-tube flapping restraint spring similar to that used in the UH-1B tests, evaluated the stability characteristics of varying spring rates. As shown in Figure 14, hover control sensitivity and damping were increased with increasing spring rate. Cockpit vibrations and oscillatory loads in the rotor and controls were insignificantly affected, but the increased mast loads due to flapping restraint limited both the magnitude of control inputs and the center of gravity range that could be investigated. Based on increased control power, a cg extension of more than one inch is possible with no change in control margins. The flapping angles were measured to have reduced as expected.

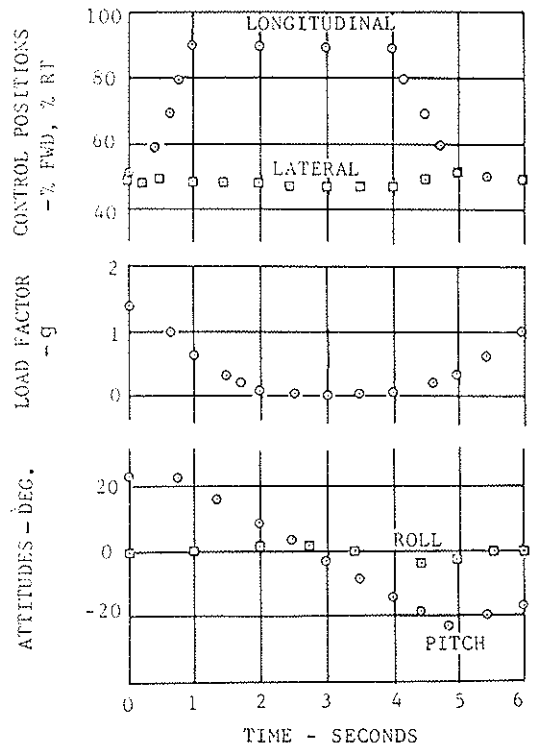

Figure 13. Model OH-58A Pushover with Elastomeric Hub Restraint at 97 Knots

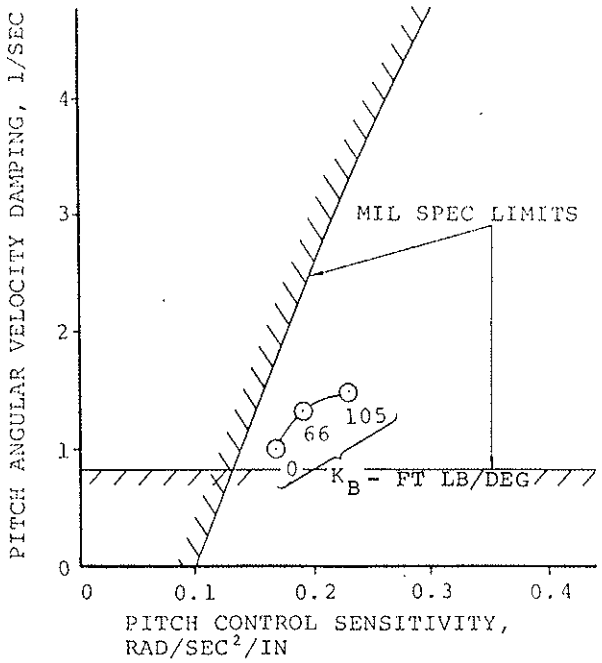

Figure 14. Effect of Hub Restraint on Hover Control Sensitivity and Damping

A favorable side effect, which is nevertheless important for light aircraft with a low rotor height above the ground, is that the rotor at low rpm and at standstill squares up with the mast, thus minimizing mast contact and rotor tip path plane excursions under high wind conditions.

IV. Rubber Hub Springs

While the steel torsion springs did work well, it was found that rubber springs could be made lighter and more compact. The use of rubber also offered the possibility of easily making the spring nonlinear, while it provided a certain amount of inherent damping. Rubber hub springs were first introduced in the three-bladed XV-15 rotor (Reference 6) and the experimental scissors rotor (Reference 7).

A linear rubber hub spring was designed for the Model 222 (Figure 15) and a nonlinear rubber hub spring for the 214ST (Figure 16). In both cases, the pilots reported a significant decrease in the pilot workload required to hover. This workload reduction arises from two sources, (1) increased control power due to the additional hub moment effect on the fuselage, and (2) the improvement in hovering dynamic stability due to the increased rotor damping.

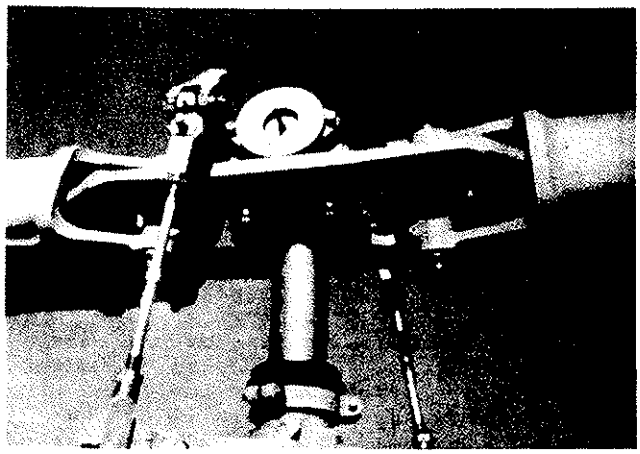

Figure 15. BHT Model 222 Hub Spring

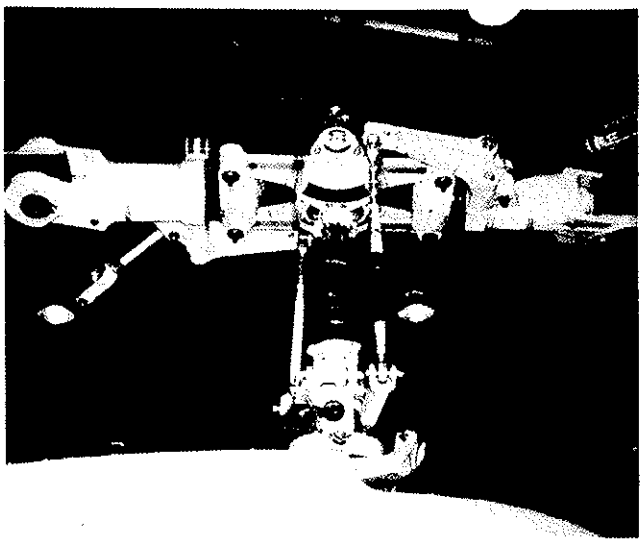

Figure 16. BHT Model 214ST Hub Spring

Increased control power due to the effect of hub restraint is evaluated by analyzing the moments producing fuselage angular acceleration due to unit control inputs. For example, in pitch:

$$\text{Control Power} = \frac{\partial(\text{Pitching Moment})}{\partial(\text{Longitudinal Cyclic Control Input})} = (Th+K_B)\frac{\partial\beta}{\partial\delta}_{F/A} \qquad (9)$$

For a helicopter with no hub restraint, the pitching moment in hover comes entirely from the thrust vector tilt produced by the control input times its moment arm, h, the height of the hub above the fuselage center of gravity. When hub restraint, K_B, is added, an increase in pitching moment (or control power) is expressed as:

$$\Delta \text{Control Power} = \frac{K_B}{Th} \times 100 \qquad (10)$$

This percent increase in control power provides a convenient way to express the hub restraint magnitude for a given helicopter at a particular weight (thrust). Increased control power allows the pilot to control the aircraft with smaller control motions and, if the control system is properly tailored, reduces the workload required to hover or perform other flight tests.

The expression for control power provides a convenient method to explain the reduction in control power in low-g flight suffered by teetering rotor helicopters. With no hub restraint, the control power is a function of main rotor thrust only. If the main rotor thrust magnitude is reduced, for example in a push-over maneuver, a reduction in control power about both the pitch and roll axes results. In high speed forward flight, which is the only practical flight condition for sustained low-g operation, the primary concern is not the reduction in longitudinal control power. Since control of the rotor tip path plane is not affected by the thrust level, longitudinal control inputs will change the rotor disk angle of attack which provides a change in thrust and thus, longitudinal control power. Lateral tilt of the rotor disk has a relatively small effect on thrust level and will not produce control moments on the fuselage unless the thrust was available initially. Lateral control power in forward flight may be expressed identically to the control power in hover, as given before in Equation 9. It is lateral control power that benefits the most from the hub restraint K_B in the low-g situation. The amount of hub restraint required to successfully fly to zero-g has not been firmly established, although test results indicate that about $K_B = .25Th$ is sufficient.

The change in hovering dynamic stability can be expressed as follows. The characteristic equation of simplified equations of motion of a hovering helicopter with centrally hinged blades and no pitch-flap coupling (δ_3) can be expressed, as in Reference 8, as a cubic equation of the form:

$$D^3 + A_2D^2 + A_1D + A_0 = 0 \qquad (11)$$

where, for longitudinal motion,

$$A_2 = g\frac{\partial a_1}{\partial V} - \left(\frac{Th}{I_{Fus}}\right)\frac{\partial a_1}{\partial q}$$

$$A_1 = 0$$

$$A_0 = g\left(\frac{Th}{I_{Fus}}\right)\frac{\partial a_1}{\partial V}$$

The solution to this equation for typical values of A_2 and A_0 will give one real and one complex pair of roots. It is shown in Reference 8 that the complex roots will always be unstable for $A_1 = 0$. The unstable complex pair gives a divergent oscillatory response whose time to double amplitude is a function of the coefficients A_2 and A_0 as shown in Figure 17.

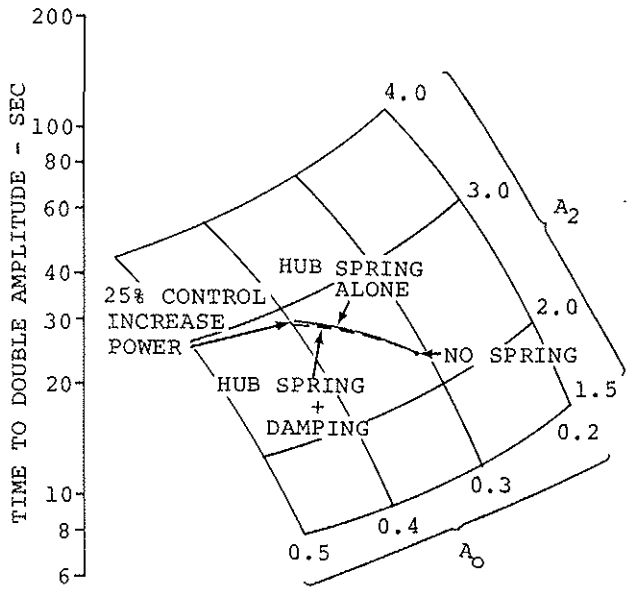

Figure 17. Effect of Elastomeric Hub Spring on Hovering Stability

The addition of hub restraint modifies the characteristic equation coefficients to decrease the instability of the hoving oscillation. The hub spring modifies both A_2 and A_0 through the addition of a spring rate term:

$$A_2 = g\frac{\partial a_1}{\partial V} - \frac{Th + K_B}{I_p}\frac{\partial a_1}{\partial q}$$

$$A_0 = g\frac{Th + K_B}{I_p}\frac{\partial a_1}{\partial V}$$

The spring provides a more powerful rate damping and speed stability effect. The effect of hub restraint on the time to double amplitude of the hover oscillation is also indicated in Figure 17.

The inherent damping of the elastomeric material used for the hub restraint will also have an effect on the hover stability. Since the damping will act 90° out of phase with the flapping response, its effect on hover stability must be analyzed from the rotor blade flapping equations. The equation of flapping for a centrally hinged rotor blade can be expressed as:

$$\ddot{\beta} + \frac{\gamma\Omega}{8}\dot{\beta} + \Omega^2\beta = f(t) \qquad (12)$$

For an elastomeric hub spring, the spring rate is included in the β term and the damping in the $\dot{\beta}$ term as:

$$\ddot{\beta} + \left(\frac{\gamma\Omega}{8} + \frac{K_B\tan\delta}{I_B\Omega}\right)\dot{\beta} + \left(\Omega^2 + \frac{K_B}{I_B}\right)\beta = f(t) \qquad (13)$$

If the pitch rate damping is to be evaluated, f(t) may be set equal to $2q\Omega\sin\Omega t$ and the change in flapping due to a unit pitch rate may be expressed as

$$\frac{\Delta a_1}{q} = -\frac{16}{\gamma^*\Omega}$$

where

$$\gamma^* = \gamma\left(1 + \frac{8K_B\tan\delta}{\gamma I_B\Omega^2}\right)$$

Thus, the effect of the elastomeric spring damping is to increase the effective Lock Number and thus to decrease the flapping-with-pitch rate derivative. This effect slightly reduces the increased pitch damping due to the hub spring but does not become a significant factor in the hovering stability equation. The effect of the elastomeric damping is also illustrated in Figure 17.

V. Nonlinear Hub Spring

The main advantages of using rubber are that it offers not only better stability and control with a lightweight design, but that the spring rate can be made nonlinear. This allows the use of a moderate hub spring stiffness at small flapping angles, thus minimizing the structural loads in the high time portion of the fatigue spectrum and reducing the gust sensitivity. In maneuvers where large flapping angles may occur, a much higher moment is available for more control power. In addition, if the nonlinearity is designed as a rubber bumper as shown in Figure 18 and 19, then hard metal-to-metal flapping stop contact can be avoided.

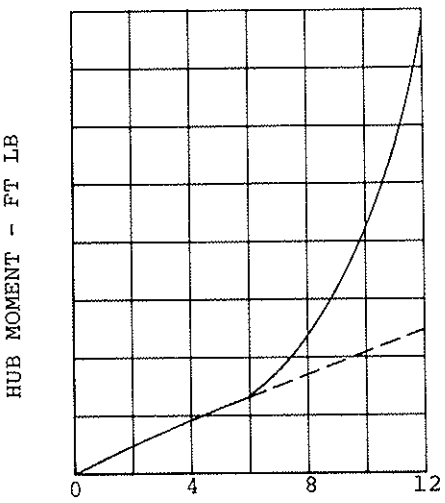

Figure 18. Nonlinear Hub Spring

The tests with the Model 214ST nonlinear rubber spring system revealed that:

(a) Vibrations were not measurably affected,
(b) Flapping in level flight and maneuvers was reduced by as much as 25%,
(c) An increase in cg travel of 1.5 inches is achieved,
(d) The low-g controllability is noticeably improved,
(e) The hover SCAS-off dynamic stability is much improved, and even SCAS-on, the pilot workload is reduced,
(f) Rotor flapping at low rpm's and with the rotor stopped is much reduced.

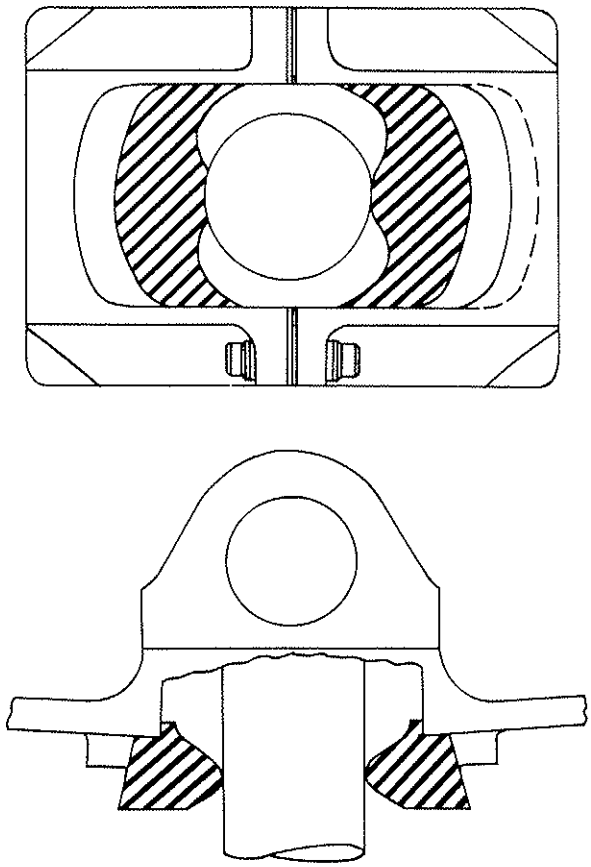

Figure 19. Nonlinear Hub Spring Design

VI. Future Possibilities

The knowledge gained through the studies discussed in the previous chapters could be applied to a hypothetical rotor in which the hub is again locked out, as in our 1961 experiment. But now flexures between the hub and the blades are introduced to provide the softness required to keep the system stable. Since there is no flapping hinge and consequently no underslinging, it is necessary to put the in-plane cantilever blade mode exactly at one per rev. This prevents the two-per-rev hub moment from vibrating the mast as discussed earlier. The oscillatory hub shears will be isolated through a nodal beam-focused pylon arrangement.

With the elimination of the flapping bearing, it is possible to design a two-bladed bearingless main rotor. In Reference 8, such a rotor concept was shown. The total number of parts of such a concept could be very small, especially if the cuff is made integral to the blade root end, as shown in Figure 20.

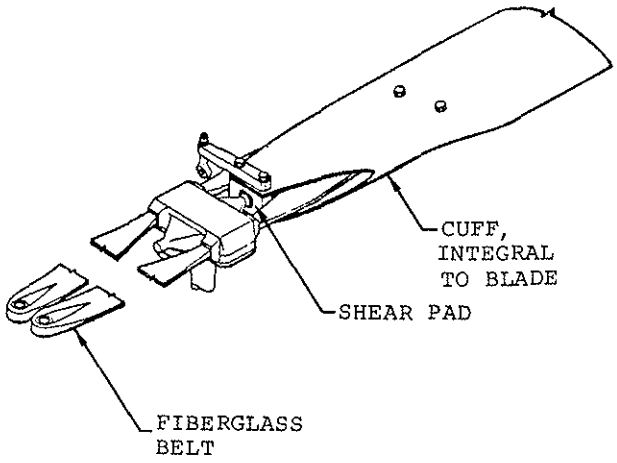

Figure 20. Two-Bladed Bearingless Main Rotor

Concluding Remarks

An overview was given of the development work that led to the application of hub springs on two-bladed rotors. The addition of such springs has shown to improve handling qualities, maneuverability, and to reduce flapping. Recently introduced rubber hub springs offer further advantages by reducing weight, metal-to-metal flapping stop contact, and by providing a nonlinear spring rate.

The vibrations expected from the hub spring have been minimized and brought under control by various means. In particular, the tuning of the inplane cantilever blade frequency to one per rev offers interesting possibilities which one day may make feasible the design of an ultra-simple two-bladed bearingless rotor design.

References

1. B. Kelley, Helicopter Technological Progress, Part II - Bell Helicopter Co., Vertiflite, Vol. 21, No. 8, Jan./Feb. 1975.

2. W.L. Cresap, Rigid Rotor Development and Flight Tests, presented at the Institute of the Aerospace Sciences Thirtieth Annual Meeting, Jan. 1962.

3. L.W. Dooley, Handling Qualities Considerations for NOE Flight, Forum Proceedings of the Thirty-Second Annual National Forum of the American Helicopter Society, May 1976.

4. J.M. Drees, Vibration Isolation Through Dynamic Coupling, presented to Aerospace Flutter and Dynamics Council, May 1973.

5. W. Sonneborn and J. Yen, Hub Moment Springs on Two-Bladed Rotors, Proceedings of the Specialists Meeting on Rotorcraft Dynamics, American Helicopter Society and NASA/Ames Research Center, Feb. 1974.

6. K.G. Wernicke and H.K. Edenborough, Full Scale Proprotor Development, Proceedings of the Twenty-Seventh Annual National Forum of the American Helicopter Society, May 1971.

7. W. Sonneborn and J. Drees, The Scissors Rotor, Proceedings of the Thirtieth Annual National Forum of the American Helicopter Society, May 1974.

8. Anon., Engineering Design Handbook, Helicopter Engineering, Part One: Preliminary Design, AMCP 706-201, U.S. Army Materiel Command, Aug. 1974.

9. D.L. Kidd, V.H. Brogdon and J. A. White, Advanced Two-Bladed Rotor Systems at Bell Helicopter Textron, Proceedings of the American Helicopter Society Mideast Region Symposium on Rotor Technology, Aug. 1976.